JTTEE5 21:176–186
DOI: 10.1007/s11666-011-9700-7
1059-9630/$19.00 © ASM International

Optimization of Plasma Spray Process Using Statistical Methods

F. Gao, X. Huang, R. Liu, and Q. Yang

(Submitted July 15, 2011; in revised form October 9, 2011)

The microstructure features of coatings produced by a plasma spray process are affected significantly by the process parameters such as powder size, spray gun nozzle size, total plasma gas flow, ratio of $H_2 + N_2$ over total gas flow, and so on. This article presents a study of the effects of these parameters on the microstructure (porosity, formation of crack, unmelted particle and oxide phase) of NiCrAlY coatings deposited by the Mettech Axial III™ System. A Taguchi array is used to design the spraying process parameters. The results of the microstructure evaluation are used to generate regression equations for the prediction of coating microstructure based on process parameters. The results predicted from the regression equations are in good agreement with the experimental results according to a confidence level of 0.95. Among the parameters examined, the powder size and the ratio of $H_2 + N_2$ over total gas flow rate are the most significant parameters affecting the occurrence of crack, porosity, unmelted particle and oxide. Within the range of the designed process parameters, lower powder size and higher ratio of $H_2 + N_2$ over total gas flow rate lead to less cracks, pores, unmelted particles but more oxides. Nozzle size has marginal influence on oxides which increase with nozzle size. Gas flow rate has no direct influence on any coating feature evaluated with the range of variation.

Keywords axial injection, crack, NiCrAlY coating, oxide, plasma spray, porosity, process optimization, regression equation, Taguchi method, unmelted particle

1. Introduction

Plasma spray is one of coating deposition processes in which molten, semi-molten or solid particles are deposited onto a substrate. It uses ionized gas to accelerate the feed powder particles while heating them at the same time. The temperature of a plasma jet depends on the degree of ionization of plasma gas and the parameters of the plasma torch. To varying degrees, all process parameters contribute to the in-flight particle temperatures and velocities during spraying and in turn influence the coating features, such as density, defects and oxide formation, deposition efficiencies, as well as distortion and stresses experienced by the coated components. Attributes of powders and powder feed conditions also play an important role in evolution of the coating microstructure. Particle temperature is an important factor determining splat spreading and solidification and subsequently the coating density, as viscosity and surface tension decrease with rising temperature. On the other hand, the higher the temperature, the more the tendency for oxide formation is. Particle velocity is another important factor in controlling density and oxidation. Melting index and oxidation index, as functions of the in-flight particle temperature and velocity, have been used to predict oxide content and porosity in the coatings and satisfactory results have been obtained (Ref 1, 2).

To develop an optimal coating, it is necessary to have a fundamental understanding of the factors that have significant effects on the in-flight particle temperature and velocity. Typical process variables for atmospheric plasma spraying include (Ref 3):

- powder shape, size and distribution;
- electric power input;
- flow rate and composition of plasma gases;
- spray distance; and
- powder feed rate.

Powder particle size and distribution determine the peak temperature and temperature distribution within powder particles and the powder velocity. It has been found that the powder temperature and velocity could be reduced up to 30% when the mean powder size changed from 25 to 75 μm (Ref 4). The heat source for plasma spray process is a high voltage DC power supply (several hundreds of kilovolts) which forms an electric arc between two electrodes within a spray gun. Plasma gas becomes ionized (plasma) when passing between the electrodes and exits the spray gun at velocities between 200 and 500 m/s. The core temperature of the ionized gas (plasma) can reach 12,000 °C (Ref 5). It is generally accepted that the

F. Gao, X. Huang, and **R. Liu**, Department of Mechanical and Aerospace Engineering, Carleton University, 1125 Colonel By Drive, Ottawa, ON K1S 5B6, Canada; and **Q. Yang**, Institute for Aerospace Research, National Research Council of Canada, 1200 Montreal Road, Ottawa, ON K1A 0R6, Canada. Contact e-mail: fgao1@connect.carleton.ca.

current is the next most important parameter for the particle temperature and velocity. Plasma gases are another important factor(s) that can affect particle temperature and velocity. Before spraying, the primary gas, usually argon, is introduced to start plasma, and then the secondary gases flow in to begin the spraying. The secondary gas can be helium, nitrogen, hydrogen or mixture of them. It is known that the primary gas flow rate strongly influences the powder particle velocity, whereas the secondary gas flow rate has effects on the average particle temperature (Ref 6). The primary gas flow rate will change after the secondary gas is introduced. The selection of secondary gases can cause significant change in the plasma gas, which in turn results in different coating features (Ref 7). Diatomic gases, such as nitrogen and hydrogen, require more energy to cause molecular dissociation and these gases absorb and possess much higher enthalpy than monatomic gases such as helium and argon. When the ionized diatomic gases encounter a relatively cold surface such as injected powder material, they recombine to form diatomic molecules and rapidly release heat at the same time. Therefore, hard-to-melt materials are easier deposited with diatomic nitrogen or a mixture of nitrogen and hydrogen than with argon or helium; whereas for easy-to-melt materials, argon or a mixture of hydrogen and argon is preferred to provide environment protection. The use of hydrogen can reduce the oxide formation. Finally, spray distance greatly influences the coating density and deposition efficiency; both of which decrease with increased spray distance. Powder feed rate is commonly regarded critical only for coating thickness control.

With the recent installation of Mettech Axial III™ plasma spray system, this study was undertaken to examine the effects of aforementioned parameters on NiCrAlY type coating microstructure features. The Mettech Axial III™ plasma spray system is a novel axial powder injection system employing three sets of electrodes. Powder is carried through the center of the powder port and ejected co-axially with the plasma gases. The advantages of this system over the conventional plasma spray system, which use radial powder injection, are (Ref 5):

- full entrainment of powder in the plasma jet, which increases deposition efficiency, and
- more thermal and kinetic energy, which enhances the density and adhesion between the coating and substrate, and reduces oxidation.

The increased kinetic energy, however, shortens the dwelling time for particles in plasma gas and increases the tendency to form unmelted particles. Therefore the size of metallic powders should not exceed 100 μm.

Since the optimization of a coating microstructure requires a full control of the numerous operating parameters, statistical methods may provide a useful tool in the design of experiments (DOE) and the interpretation of the results (Ref 3, 8, 9). DOE methodologies used in the past to optimize the air plasma spraying process can be categorized into the following groups (Ref 3):

- Hadamard or Plackett-Burman matrices;
- two-level full factorial designs or two-level fractional factorial designs;
- response of surface methodology (RSM) designs; and
- Taguchi Method.

The Hadamard matrix has been used to screen a great number of factors (more than 4 factors) that may potentially influence the response. Each factor has two levels. The resulted regression equation is a first order polynomial and the interaction terms are not taken into account. Two-level factorial designs are used when interactions between factors are considered. The purpose of the fractional factorial design is to extract part of experiments from the full factorial design while enables the realization of main effects of variables. When relationship between the response and factors are not linear or the factors are at higher levels, RSM design must be used to determine quadratic or cubic terms. Taguchi method is a statistical technique developed by Genichi Taguchi to improve the quality of manufactured goods, and more recently found wide applications in engineering design and optimization. One of the advantage of using Taguchi method on DOE is to minimize experimental runs using saturated fractional factorials for two-level screening designs or three-level designs. Methods for determining the significance of the regression coefficients include analysis of variances, normal plot and the Student-test. To optimize the plasma spray process and develop empirical equations for process control in this study, Taguchi method was implemented for the design and evaluation of spraying parameters for the newly installed Axial III plasma system and analysis of variances was used to analyze the experimental results.

2. Experimental Procedure

2.1 Coating Materials and Substrate

Three different commercially available spherical, gas atomized powders were used in this study. The nominal composition and powder size for each powder are listed in Table 1. 304 stainless steel substrates were cut to a standard size of 25 × 100 mm^2 and grit blasted to form clean and rough surfaces within 2 h before spraying. The surface roughness, R_a, ranges from 2.5 to 3.0 μm for all samples produced in this study.

2.2 Plasma Spraying Process Parameters

Parameter selection was based on previous research by the author, and the current and standoff distance were

Table 1 Powder parameters and powder feed rate

Powder	Powder size, μm	Composition, %
NI-246-4	−90/+38	Ni-31Cr-11Al-0.1Y
NI-164-2	−75/+45	Ni-22Cr-10Al-1Y
NI-343	−45/+10	Ni-22Cr-10Al-1Y

Table 2 L9 Taguchi matrix and process parameters

Coating	Powder	Maximum powder size, mm × 10^{-3}	Nozzle, mm	Total flow rate, sl/min	Voltage, V	H_2, %	N_2, %	Ar, %
1-1	NI-246-4	0.090	12.7	300	169	30	10	Bal.
1-2			11.1	265	148	23		
1-3			9.5	230	134	16		
1-4	NI-164-2	0.075	12.7	265	145	16		
1-5			11.1	230	141	30		
1-6			9.5	300	167	23		
1-7	Ni 343	0.045	12.7	230	137	23		
1-8			11.1	300	169	16		
1-9			9.5	265	149	30		

Table 3 Constant process parameters

Current, A	Standoff distance, mm	Duration of spray, min	Preheat cycle
250	150	2	5

held constant at 250 A and 150 mm respectively due to the fact that these two parameters have less influence on coating features than other parameters for the Mettech Axial III™ System (Ref 10). A L9 Taguchi DOE matrix, as shown in Table 2, was designed to systematically vary the settings of the following four parameters: powder size, diameter of nozzle, total flow rate of plasma gas, and the ratio of $H_2 + N_2$ over total gas. The voltage values which are dependent on the current and total gas flow rate, were listed in Table 2. Coatings were applied using a Mettech Axial III™ System at a powder feed rate of 40-50 g/min. The specimens were clamped onto a turn table with a rotational speed of 220 rpm and vertical motion speed of 17 m/s. Argon gas was used as the primary gas at a flow rate of 225 sl/min and powder carrier gas at 12 sl/min. Hydrogen (H_2) and nitrogen (N_2) gas mixture was employed as the secondary gas for spraying. The total amount of primary argon varied with the introduction of the secondary gas change in total gas flow rate (the total gas flow consisted of the varied argon, and the secondary hydrogen and nitrogen). An additional test was conducted to verify the validity of the empirical equations derived from the first set of experiments which are detailed in Table 2 and the process repeatability. The additional test parameters are listed in Table 3.

2.3 Coating Characterization

Fixed nominal coating thickness for all samples was attempted by electronically controlling the spray time. The coated specimens were sectioned using a diamond saw and then mounted in bakelite. The specimens were ground using 320-1200 grit SiC papers followed by 6, 3, and 1 μm diamond suspensions and finished with 0.05 μm silica suspension. The microstructure characterization was performed using a Philips XL 30 SEM to obtain micrographs of the coatings. SEM images of as-polished cross sections of the coatings are shown in Fig. 1. Although similar spray time was used, the deposition efficiency varied from run to run due the changes in other process parameters such as nozzle size and flow rates. As such, some coatings, for example coating 1-3 and coating 1-4, are thinner than the others due to the low deposition efficiency. EDS mappings (of Al and O) were used to distinguish pores (lack of intensity of any element) and oxides (enriched in Al), as shown in Fig. 2. In particular, three discernable levels of contrast were identified. The darkest region in Al map is identified as pores (some small pores were accompanied with oxides) while brightly contrasted region in Al maps is oxides. The intermediate contrasted region represents the bulk of coatings and lastly the unmelted particles are shown as spherical particles. Image analysis software (Clemex Technologies Inc. Canada) was used to determine the percentage of porosity, unmelted particles and oxide phases in the coatings based on their area fractions. Three SEM images at 500× taken at various locations on each coating specimen were imported to the image analysis program. For thinner coatings, the images had to be further enlarged for capturing similar amount of image field.

2.4 Regression Analysis

Theoretically, the measured percentages of crack, porosity, unmelted particle and oxide can be considered as the response functions of the four process parameters investigated in this study. Polynomial equations of the four process parameters can be expressed as (Ref 11):

$$F(x_1,x_2,x_3,x_4) = A + \sum_{i=1}^{4} x_i + \sum_{i=1}^{4}\sum_{i<j}^{4} x_i x_j + \cdots + \sum_{i=1}^{4}\sum_{i<j}^{4} x_i^{m-1} x_j^{m-1} + \sum_{i=1}^{4} x_i^m \quad \text{(Eq 1)}$$

where A is a constant, $F(x_1, x_2, x_3, x_4)$ stands for the percentage of crack, porosity, unmelted particle and oxides, x_1, x_2, x_3, x_4 are powder size, nozzle size, total gas flow rate, the ratio of H_2 plus N_2 over total gas flow rate, respectively, and m is the order of the polynomial equation. The larger the exponent m, the more accurate the polynomial equation is. However, a value of m equivalent to one is generally used to simplify the calculations and analysis. In the present analysis, m values from one to two were used to generate the equations and the results were compared.

After the crack, porosity, unmelted particle and oxide data of the experimental trials were obtained, the

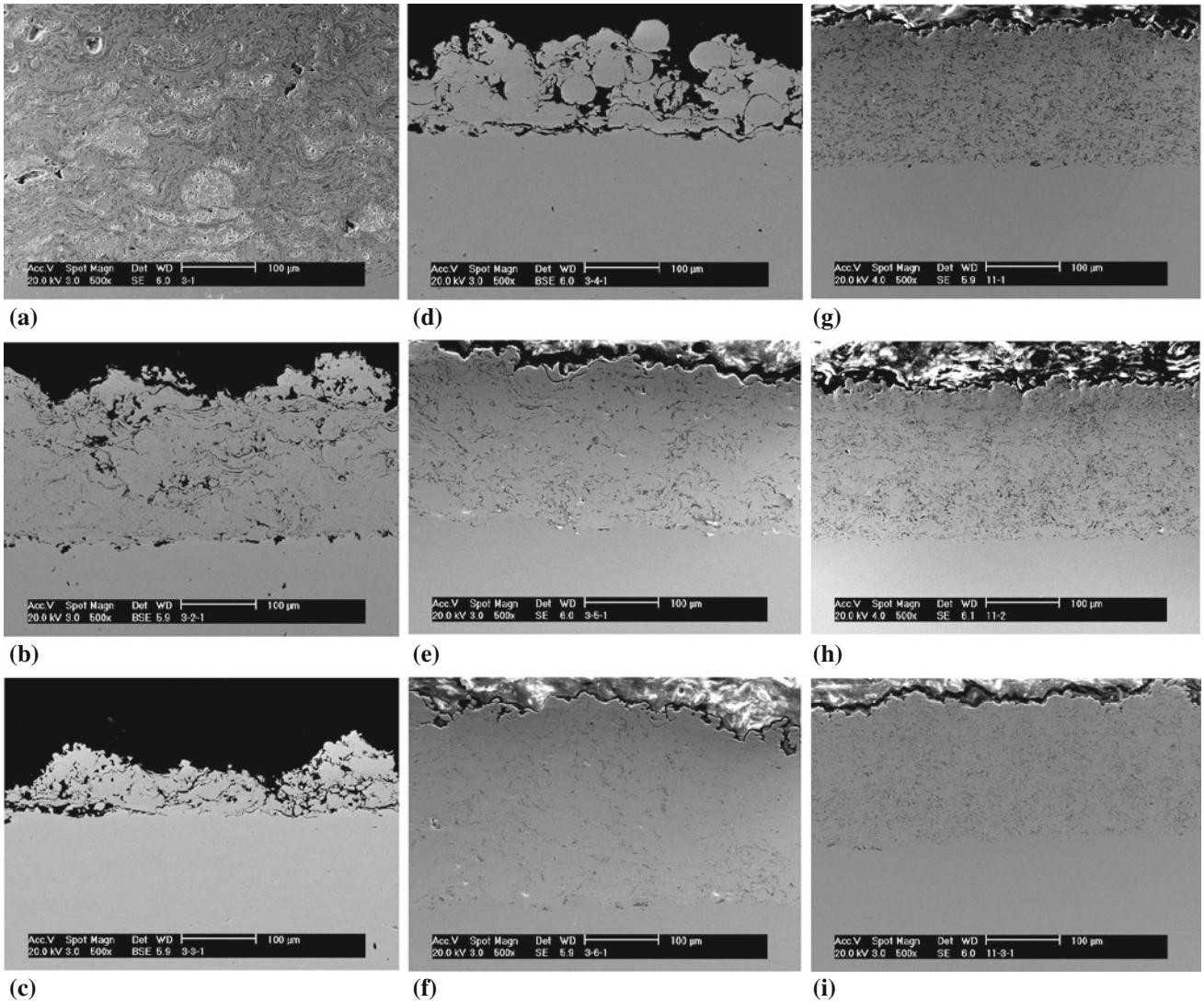

Fig. 1 Microstructures of the coatings from the first set of experiments. (a) Microstructure of coating 1-1. (b) Microstructure of coating 1-2. (c) Microstructure for coating 1-3. (d) Microstructure for coating 1-4. (e) Microstructure for coating 1-5. (f) Microstructure for coating 1-6. (g) Microstructure for coating 1-7. (h) Microstructure for coating 1-8. (i) Microstructure for coating 1-9

polynomial equations related to the investigated process parameters were generated by regression analysis. However, nine trials, shown in Table 2, were insufficient to conduct a regression of the experimental results with an order of more than one in a regression equation. Therefore the variables in the regression equation must be shifted using statistical testing to eliminate the terms that influence the response functions negligibly, and retain only those statistically significant to the response function. In the present investigation, a stepwise regression method was used. It started with a simple model and gradually more parameters higher orders of parameters and their interactions were incorporated until the model became significant.

An effective regression equation should meet the following requirements (Ref 12): a high confidence level, the effectiveness of the regression equation and error prediction. The confidence level could be determined from the Fisher value of the regression freedom (m), as the numerator, and the residual degrees (n), as the denominator of the corresponding regressed equation. α is the critical value for an F distribution, which usually is 0.05. If the Fisher value (F-value) of the regressed equation is larger than a threshold F-distribution value, $F(m, n, 1 - \alpha)$, its confidence level would be higher than $1 - \alpha$ (where α is the critical value for an F distribution, and usually set around 0.05). The threshold value, $F(m, n, 1 - \alpha)$, can be found in most statistics computational resources when the numerator, denominator and α values are given (Ref 11).

The effectiveness of a regression equation can also be determined by the coefficient of determination, R^2, of the regression equation (Ref 13, 14). This coefficient describes the percentage of the response variation that the equation can account for, i.e., it is a statistical measure of how well the regression line approximates the real data points. The

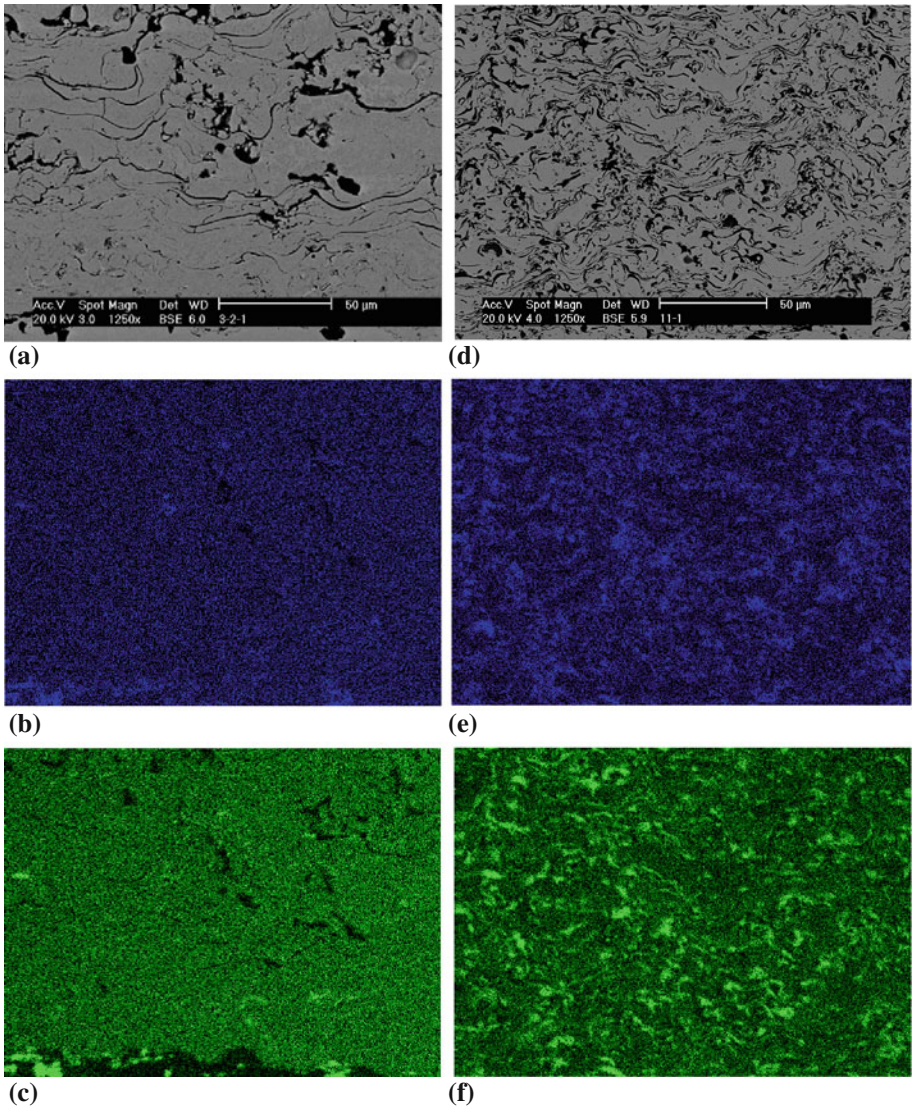

Fig. 2 EDS mapping images for coating 1-2 and 1-7. (a) SEM image of coating 1-2. (b) O mapping of coating 1-2. (c) Al mapping coating 1-2. (d) SEM image for coating 1-7 at high magnification. (e) O mapping for coating 1-7. (f) Al mapping image coating 1-7

general acceptable value of R^2 is 75% (Ref 15). The proper prediction of error should be consistent with the reliability of the experimental data, i.e., the predicted error should be within certain confidence interval of the experimental data. The predicted error of the equation can be measured by the residual mean square value. For example, if the process parameters were x_1, x_2, x_3 and x_4, there would be a probability of $1 - \alpha$ that the predicted response function is among $F(x_1, x_2, x_3, x_4) \pm 2 \times (\text{residual mean square})^{1/2}$ (Ref 12). The confidence intervals of the measured data at 1-α confidence level were calculated by the following formula:

$$F = \bar{F} \pm t(1 - \alpha/2, n) \times \sqrt{\text{MSE}} \quad \text{(Eq 2)}$$

where $\bar{F}$ is mean value of response functions, $t(1 - \alpha/2, n)$ is 100 $(1 - \alpha/2, n)$ percentile of the t distribution with n degrees of freedom, and MSE is residual mean square.

3. Results and Discussion

3.1 Microstructures of Coatings

The specimens were designated coating 1-1 to coating 1-9 according to the spraying parameters assigned. As seen in Fig. 1, NiCrAlY coatings have a typical splat microstructure with porosities, oxides and unmelted particles. Cracks are observed in some coating specimens (Fig. 1c, d) at the coating/substrate interface. The amounts of cracks, porosities and unmelted particles vary significantly with the powder size and other process parameters. The microstructure of the as-sprayed NiCrAlY coating contains single β-NiAl phase (with a fraction of dissolved chromium) when Cr content is 32% in Ni 246, whereas the NiCrAlY coating is composed of β-NiAl + γ(Ni)/γ′(Ni_3Al) when Cr content is 22% in Ni 164 and 343. (The influence of process parameter and original powder composition on

phase compositions will not be discussed in this communication.)

3.2 Regression Equation Derivation

The quantitative results for four coating features (percentage of cracks at the interface, percentages of porosity, unmelted particles and oxides) are summarized in Table 4. Based on the results, the influences of each spraying process parameter on these coating features are illustrated in Fig. 3.

Table 4 Percentages of crack, porosity, unmelted particle and oxide in the coatings

Coating	Crack at interface, %	Porosity(a), %	Unmelted particles, %	Oxide, %
1-1	40	8.17	6.10	2.87
1-2	56	10.83	10.30	1.10
1-3	100	20.84	45.00	0.00
1-4	100	18.06	15.35	0.00
1-5	0	7.70	4.40	6.77
1-6	0	5.20	12.13	4.50
1-7	0	5.10	0.00	12.67
1-8	0	4.80	2.93	8.73
1-9	0	4.00	0.00	14.20

(a) Measured based on area percentage of pores over total area analyzed

The four process parameters along with their quantitative measures used in regression equations are given in Table 5. The influences of parameters on coating features cannot be accurately predicated using simple linear regressions based on the curves in Fig. 3. Therefore the combination of process parameters (such x_1x_2, x_1x_3, x_3x_4) and higher orders of these process variables (such as x_1^2) need to be incorporated into the regression equation in order to correlate the parameters with the coating features more accurately.

A stepwise regression analysis started with a simple linear regression model for the powder size, which is illustrated in Table 6. A set criterion, $p = 0.65$, was applied for removing and adding parameters. Some parameters were eliminated if p value was too low. In each step the parameters were added in the equation when the p values of the parameters were greater than 0.65, and the parameters were removed from the equation when the p values of the parameters were less than 0.65. Meanwhile the standard deviation (S) and coefficient of determination (R^2) were also calculated and included in Table 6. These parameters remained in last iteration step made up the regression equations for all four coating features

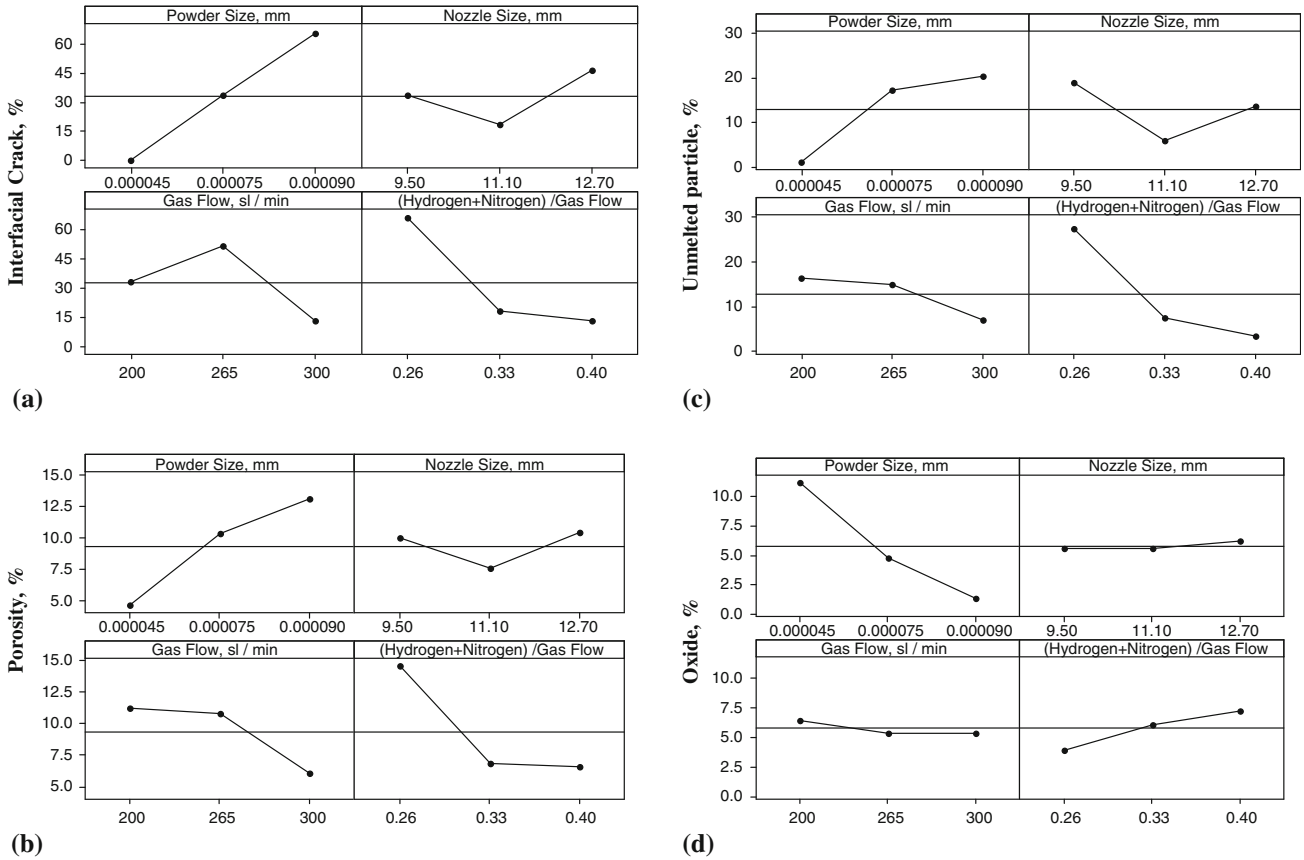

Fig. 3 Results of the experiments for the Taguchi matrix. (a) Influences of spraying process parameters on cracking. (b) Influence of spraying process parameters on porosity. (c) Influence of spraying process parameters on unmelted particles. (d) Influence of spraying process parameters on percentage of oxide

summarized in Table 7. Also included in this table are other statistic values such as S, R, F, m, n, and p value as well as RSS and MSE. RSS represents residual sum of squares. All regression equations have five degree of freedom (m) and residuals have three degrees of freedom (n).

In the polynomial equations containing the process parameters investigated in this study, the all F values (Fisher value) in Table 7 are greater than the threshold $F(5, 3, 0.95) = 9.01$. In all cases R^2 values are over 96 %, which indicate that less than 4% of the total variations are not explained by the regression relationships. Thus, it can be concluded that the regression equations are all significant. It should be noted that x_3 (total gas flow rate) has not been included in the regression equations due to its insignificant influence.

Table 8 compares the measured results of the coating features from the experiment with the values calculated from the regression equations. The calculated values agree well with the experimental results and the predicted errors fall into the confidence interval of the measured data at 95% confidence level ($\alpha = 0.05$).

Table 5 Values for x_1, x_2, x_3 and x_4 used in regression equation

x_1, maximum powder size in mm $\times 10^{-6}$	x_2, nozzle size in mm	x_3, total flow rate at sl/min	x_4, ratio of $H_2 + N_2$ over total gas
90	12.7	300	0.40
75	11.1	265	0.33
45	9.5	230	0.26

4. Discussion

4.1 Significance of Parameters on Coating Features Characterized by Statistical Analysis

Table 9 summarizes the effects of the process parameters on the microstructural features of the coatings based on the regression equations. It is generally accepted that the spray parameters could be ranked based on their p values on coating features (Ref 4) and accordingly the ranking was made as shown in Table 9. All parameters are categorized into three levels: the most significant, medium significant and least significant. The most significant process parameters found in this study are the particle size (x_1), the ratio of $H_2 + N_2$ over total gas (x_4), their interaction (x_1x_4) and their squared values (x_1^2 and x_4^2). The next important parameters are nozzle size (x_2) and parameters related to the nozzle size.

The sequential sums of squares (SS) for parameters included in regression equations (Table 8) can be quantitatively calculated to provide comparison of the significance of various parameters on coating microstructural features. The sequential SS measures the reduction in the

Table 6 Procedures of stepwise regression analysis for porosity

Parameter and statistical values	Step 1	Step 2	Step 3	Step 4	Step 5
A	−3.84	−3.84	−21.10	−50.31	13.53
x_1	1.88×10^5	4.81×10^5	9.28×10^5	1.24×10^6	1.14×10^6
$p(x_1)$	0.111	0.072	0.036	0.134	0.769
x_1x_4		-8.86×10^5	-2.24×10^6	-3.19×10^6	-2.84×10^6
$p(x_1x_4)$		0.015	0.054	0.012	0.006
x_4^2			154	254	7.61×10^2
$p(x_4^2)$			0.177	0.033	0.018
x_2				1.53	1.38
$p(x_2)$				0.068	0.026
x_4					-3.60×10^2
$p(x_4)$					0.047
S	4.57	4.10	3.01	2.62	1.11
R^2	72.24	72.15	87.98	93.19	98.75

Table 7 Regression equations for four coating microstructure features

Feature	Regression equations	S	R^2	F	m	n	p	RSS	MSE
Crack	$C(x_1, x_2, x_3, x_4) = -3.00 + 7.78 \times 10^6 x_1 - 1.88 \times 10^3 x_4 - 1.96 \times 10^7 x_1x_4 + 0.57x_2^2 + 4.35 \times 10^3 x_4^2$	11.78	97.21	21.03	5	3	0.015	14584.70	138.73
Porosity	$P(x_1, x_2, x_3, x_4) = 13.53 + 1.14 \times 10^6 x_1 + 1.38x_2 - 3.60 \times 10^2 x_4 - 2.84 \times 10^6 x_1x_4 + 7.61 \times 10^2 x_4^2$	1.11	98.73	47.35	5	3	0.005	293.79	1.24
Unmelted particle	$U(x_1, x_2, x_3, x_4) = 49.00 + 3.32 \times 10^{-6} x_1 - 8.53 \times 10^2 x_4 - 5.84 \times 10^7 x_1x_4 - 7.13 \times 10^{-9} x_1^2 + 1.65 \times 10^3 x_4^2$	4.69	96.72	22.01	5	3	0.005	1989.45	22.72
Oxide	$O(x_1, x_2, x_3, x_4) = -5.50 + 1.42 \times 10^5 x_1 + 0.44x_2 + 43.4x_4 - 0.87x_1x_2 - 6.80 \times 10^{-2} x_2^2$	0.87	99.01	59.59	5	3	0.003	224.40	0.75

Table 8 Comparison of the experimental results with the values calculated from the regression equations

	Crack at interface, %				Porosity, %			
Coating	*E*-value(a)	*C*-value(b)	Predicted error	Confidence interval at 95%	*E*-value	*C*-value	Predicted error	Confidence interval at 95%
1-1	39.15	34.80	16.44-63.56	2.55-77.45	8.17	8.62	5.94-10.4	4.63-11.71
1-2	56.36	45.80	32.44-79.56	18.55-93.45	10.30	10.64	8.07-12.53	6.76-13.84
1-3	100.00	100.00	76.44-100.00	62.55-100.00	20.84	20.11	18.61-23.07	17.30-24.38
1-4	100.00	100.00	76.44-100.00	62.55-100.00	18.06	18.70	15.83-20.29	14.52-21.60
1-5	0	12.57	0.00-23.56	0.00-37.45	7.70	8.57	5.47-9.93	4.16-11.24
1-6	0	5.78	0.00-23.56	0.00-37.45	5.20	5.61	2.97-7.43	1.66-8.74
1-7	0	4.42	0.00-23.56	0.00-37.45	5.10	4.36	2.87-7.33	1.56-8.64
1-8	0	0.00	0.00-23.56	0.00-37.45	4.80	4.89	2.57-7.03	1.26-8.34
1-9	0	0.00	0.00-23.56	0.00-37.45	4.00	4.68	1.77-6.23	0.46-7.54

	Unmelted particles, %				Oxide,%			
Coating	*E*-value	*C*-value	Predicted error	Confidence interval at 95%	*E*-value	*C*-value	Predicted error	Confidence interval at 95%
1-1	6.10	4.30	0.00-15.63	0.00-21.26	2.87	2.39	1.13-4.61	0.10-5.64
1-2	10.30	15.07	0.77-19.83	0.00-25.46	1.10	0.74	0.00-2.84	0.00-3.87
1-3	45.00	44.78	35.47-54.53	29.84-60.16	0.00	0.00	0.00-1.74	0.00-2.77
1-4	15.35	31.92	5.82-24.88	0.19-30.51	0.00	0.69	0.00-1.74	0.00-2.77
1-5	4.40	3.70	0.00-13.93	0.00-19.56	6.77	7.37	5.03-8.51	4.00-9.54
1-6	12.13	9.72	2.60-21.66	0.00-27.29	4.50	5.30	2.76-6.24	1.73-7.27
1-7	0.00	0.00	0.00-9.53	0.00-15.16	12.67	12.47	10.93-14.41	9.90-15.44
1-8	2.93	6.20	0.00-12.46	0.00-18.09	8.73	8.48	6.99-10.47	5.96-11.50
1-9	0.00	2.50	0.00-9.53	0.00-15.16	14.20	13.96	12.46-15.94	11.43-16.97

(a) *E*-value: Experimentally measured value. (b) *C*-value: Calculated value from regression equation

Table 9 Effects of process parameters on coating features

	p value and rank							
Process parameter	Crack at interface	Rank	Porosity	Rank	Unmelted powder	Rank	Oxide %	Rank
x_1	0.012	1	0.004	1	0.060	2	0.465	3
x_2	0.000		0.026	4	0.000	…	0.955	5
x_4	0.204	5	0.042	5	0.165	4	0.006	1
x_1x_2	0.000	…	0.000	…	0.000	…	0.105	2
x_1x_4	0.020	2	0.006	2	0.029	1	0.000	…
x_1^2	0.000	…	0.000	…	0.419	5	0.000	…
x_2^2	0.036	3	0.000	…	0.000	…	0.797	4
x_4^2	0.083	4	0.018	3	0.096	3	0.000	…

residual sums of squares (RSS) provided by each additional parameter in the regression equation. If the sequential SS of a parameter substantially reduces the residual sums of squares in a regression equation, this parameter becomes significant in the equation. Based on the percentage of the sequential sums of squares over total sums of squares for each parameter (Table 10), Pareto diagrams are generated to analyze the impact of various process parameters, as shown in Fig. 4. Pareto diagrams are simple bar charts that rank related process parameters in decreasing order of significance. (The principle of Pareto diagram is based on the unequal distribution of things in the universe. It is the law of the ''more important few versus the trivial many''; Ref 16.) By graphing each coating feature with respect of the sequential SS for all process parameters, the most significantly parameter could be identified.

Examining Table 10, it is found that over 80% of sequential SS is accumulated from the sequential SS of particle size (x_1), the ratio of $H_2 + N_2$ over total gas (x_4), and parameters related to them. This suggests that powder particle size and the ratio of $H_2 + N_2$ over total gas are the most dominating factors for all coating microstructural features. Within the range of the experimental parameters used in this study, lower powder size and higher ratio of $H_2 + N_2$ over total gas reduce the percentages of cracks, pores, unmelted particles but increase the percentage of oxides. Nozzle size has certain influence on oxides. The

Table 10 Sequential sums of squares of process parameters on coating features

Process para-meter	Crack at interface		Porosity		Unmelted powder		Oxide	
	Sequential SS	%	Sequential SS	%	Sequential SS	%	Sequential SS	%
x_1	6202.02	42.5	111.82	38.06	633.97	31.55	180.60	80.47
x_2	0.00	0.00	0.28	0.10	0.00	0.00	1.66	0.74
x_4	4266.70	29.5	94.65	32.22	873.63	43.48	38.05	16.95
x_1x_2	0.00	9.44	0.00	0.00	0.00	0.00	4.05	1.80
x_1x_4	1376.20	0.00	59.24	20.16	350.96	17.47	0.00	0.00
x_1^2	0.00	6.24	0.00	0.00	19.87	0.99	0.00	0.00
x_2^2	1829.60	12.5	0.00	0.00	0.00	0.00	0.06	0.03
x_4^2	910.20	0.00	27.80	9.46	130.90	6.51	0.00	0.00
Total SS	14584.70		293.79		2009.23		224.43	

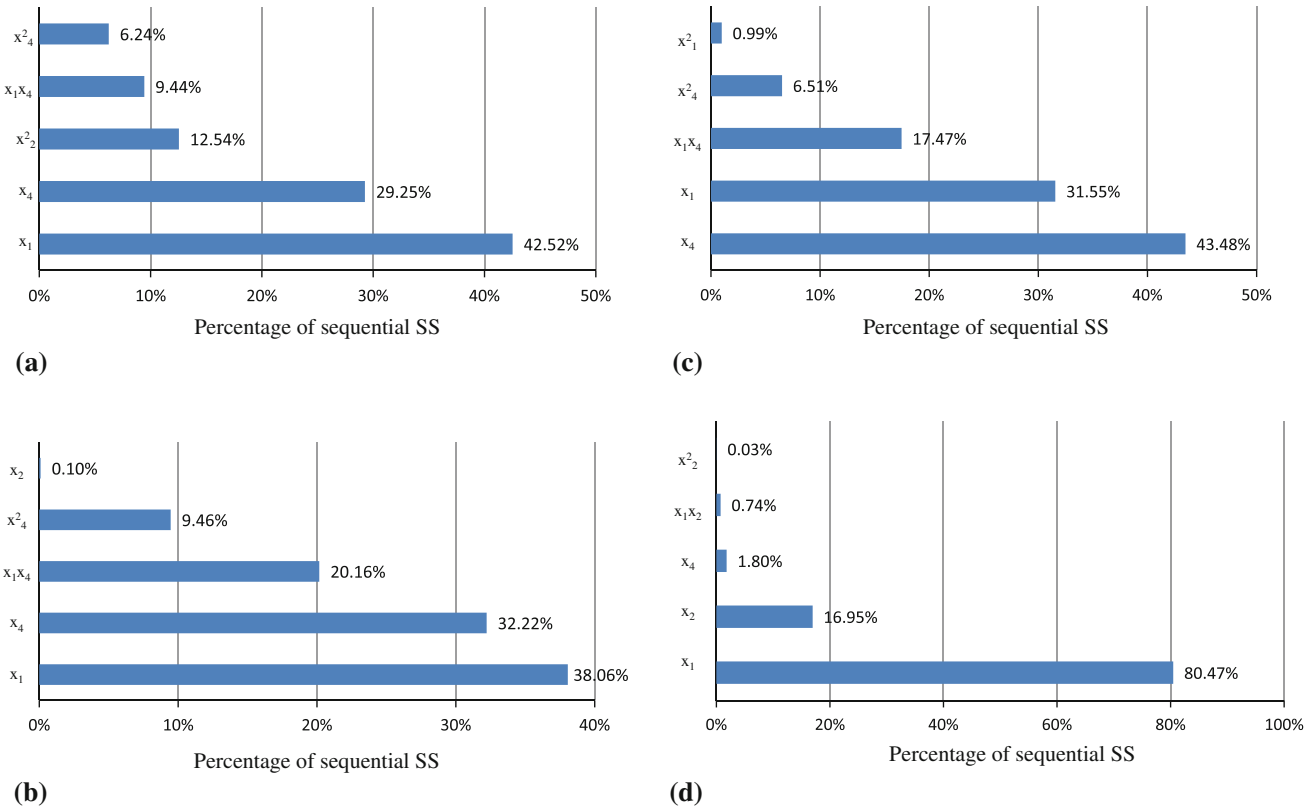

Fig. 4 Pareto diagrams showing the effects of process parameters on coating features. (a) Effects of various process parameters on cracking. (b) Effects of various process parameters on porosity. (c) Effects of various process parameters on unmelted particle. (d) Effects of various process parameters on percentage of oxides

trend observed from percentage of SS also coincides with that found from the graphic illustrations of Fig. 4(d).

4.2 Effect of Plasma Spray Parameters on Coating Features

The effects of the process parameters on the coating features are realized through the influence on the powder particle velocity and temperature. In order to understand the particle melting process, the influences of the parameters on the particle flight time, flame temperature and heat transfer coefficient should be taken into consideration. In general, a better melting is expected if more heat is convectively transferred to the particles, which suggests that the particles are easier to be melted in the plasma gas with higher flame temperature and heat transfer coefficient in addition to longer residence time.

Previous study has attempted to characterize the behavior of the particle flow in axial injection plasma torch (Ref 5, 16). Based on the results, the reasons that powder size has the most significant influence on melting status of particle can be described as follows:

(1) Temperature is uniform across the particle stream and the particle velocity can reach 380-550 m/s near torch axis. Therefore at the beginning most particles penetrate the flame center easily and the temperature of the particles increases during spraying. The particle trajectory and velocity within the plasma flame are then determined by the mass and the size of the particles. Small particles may be vaporized prior to reaching the substrate, whereas large particles may not be completely melted upon impact or miss the target entirely. Accordingly only a fraction of the particles can reach the substrate to form the coating and the ranges of the size of particles that form the coating are very narrow (Ref 17).
(2) Heat transfer coefficient increases with decreasing powder size.
(3) The enthalpy for melting a large particle, which depends on volume of the particle (assuming constant heat capacity and density), is much more than that for melting a small particle.

Small particles are more likely to be melted than large particles; this apparently decreases the tendency of forming unmelted particles and porosities. However small particles are prone to being oxidized due to the large surface-to-volume ratio. The influence of particle size on coating cracking may be likely due to the fact that the residual stress between the coating and the substrate varies with particle size. In plasma spraying, residual stress arises due to the quenching stress during solidification of molten particles and thermal stress because of differences in coefficients of thermal expansion (CTE) between the coating and the substrate (Ref 1). Other parameters may also affect the residual stress level such as preheat temperature, sand blasting before spraying (Ref 18), phase transformation (for ferrous and precipitation hardenable alloys). In this research, the thermal mismatch between the coating and the substrate is very small due to the fact that the coating and the substrate are nickel based, therefore the residual stress mainly results from the quenching stress, which relates to the solid shrinkage of splats during solidification and the restraint between splats. The large splats, produced by large particles, create more solid shrinkage than small splats, and the restraint between large splats is stronger than that between small splats. Therefore the coating produced by large particles has tendency to micro-cracking and micro-crack-induced delamination.

The ratio of $H_2 + N_2$ over total gas flow affects powder particle temperature via plasma enthalpy and heat transport (Ref 10). Higher plasma enthalpy is associated with higher ratio of $H_2 + N_2$ over total gas flow as both of these diatomic gases transfer heat to the particles more efficiently than argon. As a result the particles in the plasma stream with higher ratio of $H_2 + N_2$ experience higher in-flight temperature (Ref 7).

Nozzle size has certain effects on particle velocity and the shape of the plasma flame (Ref 5). The particle velocity decreases and the shape of the plasma flame becomes broader when nozzle size increases, and thus the residence time of the particle in the plasma stream increases. The longer residence time, consequently high particle temperature, helps to eliminate cracks, pores and unmelted particles; however, lower particle velocity promotes the formation of cracks and pores due to low kinetic energy of the particle and the formation of unmelted particles since some particles move away from the hot core of the plasma jet. The combination of these two factors results in the parabolic shaped curves for the percentages of cracks, pores and unmelted particles as a function of nozzle size as in Fig. 4(a)-(c). Whereas the curve for the percentage of oxides is almost a straight line (Fig. 3d) because both low particle velocity and broaden plasma flame promote oxidation. As such nozzle size has been found to have more influence on the formation of oxides than on the other coating features, which is further illustrated in Fig. 4(d).

Gas flow rate, to certain extent, should have influence on the particle velocity and coating features related to particle velocity, particularly porosity. However the influence of total gas flow rate was not observed within the range of variation in this study, and this could in part due to the near sonic velocity of the plasma stream generated in Mettech Axial III™ System. Therefore the total gas flow rate and its related parameters were not included in any regression equation.

4.3 Validity of the Regression Equations

The regression equations obtained from section 3.2 were validated with another experiment using the process parameters listed in Table 11. The experimental results of four key microstructure features were compared to the

Table 11 Spray trial used to assess the validity of the regression equations

Process parameter	Code	Value	Coating feature	*E*-value(a), %	*C*-value(b), %	Relative error, %
Powder size, μm	x_1	45	Crack, %	0.00	0.00	0.00
Nozzle size, in	x_2	0.38	Porosity, %	4.10	3.60	12.19
Gas flow rate, sl/min	x_3	230	Unmelted particles, %	5.23	5.46	−4.4
Ratio of $H_2 + N_2$ over total gas, %	x_4	26	Oxide, %	7.80	7.12	8.72

(a) *E*-value: Experimentally measured value. (b) *C*-value: Calculated value from regression equation

values calculated from the regression equations (Table 11). The differences between the experimental results and the calculated values are quite minimal, confirming the validity of the regression equations.

5. Conclusions

The effects of four plasma spray process parameters (powder size, ratio of $H_2 + N_2$ over gas flow, gas flow rate, and nozzle size) on the percentages of cracks along coating/substrate interface, porosity, unmelted particles and oxides in NiCrAlY coatings have been investigated in this study. A Taguchi array was used to design the plasma spray process parameters. The results for evaluating four coating features were used to create regression equations capable of predicting the microstructure based on the process parameters. The established regression equations were in good agreement with the experimental data and had a confidence level over 0.95. These equations were further employed to predict the microstructure of coating sprayed after the initial trial. The differences between the calculated and experimentally obtained results were less than 12%.

Among the parameters examined, the powder size and ratio of $H_2 + N_2$ over total gas flow rate are the most significant parameters affecting the percentages of crack, porosity, unmelted particle and oxide. Within the range of the designed process parameters, lower powder size and higher the ratio of $H_2 + N_2$ over total gas flow rate result in less cracks, pores, and unmelted particles but more oxides. Increasing nozzle size marginally increases the occurrence of oxides. Gas flow rate has no influence on any coating feature evaluated. Further study is underway to generate process index combining all process parameters into single value and relate this value to coating microstructure.

Acknowledgments

The authors are grateful to Mr. Fred Barrett for spraying all specimens and to Mr. Yunfen Qian for his help in the preparation of the metallographic samples.

References

1. S. Sampath, X.Y. Jiang, J. Matejicek, L. Prchlik, A. Kulkarni, and A. Vaidya, Role of Thermal Spray Processing Method on the Microstructure, Residual Stress and Properties of Coatings: an Integrated Study for Ni-5 wt.% Al Bond Coats, *Mater. Sci. Eng. A*, 2004, **364**, p 216-231
2. H. Xiong, L. Zheng, L. Li, and A. Vaidya, Melting and Oxidation Behavior of In-Flight Particles in Plasma Spray Process, *Int. J. Heat Mass Transfer*, 2005, **48**, p 5121-5133
3. C. Pierlot, L. Pawlowski, M. Bigan, and P. Chagnon, Design of Experiments in Thermal Spraying: A Review, *Surf. Coat. Technol.*, 2008, **202**, p 4483-4490
4. F. Azarmi, T.W. Coyle, and J. Mostaghimi, Optimization of Atmospheric Plasma Spray Process Parameters using a Design of Experiment for Alloy 625 Coatings, *J. Therm. Spray Technol.*, 2008, **17**, p 144-156
5. W.H.W. Wo, ''Heat Transfer Analysis of the Plasma Spray Deposition Process,'' Ph.D. thesis, University of British Columbia, 1997
6. V. Srinivasan, A. Vaidya, T. Streibl, M. Friis, and S. Sampath, On the Reproducibility of Air Plasma Spray Process and Control of Particle State, *J. Therm. Spray Technol.*, 2006, **15**, p 739-743
7. J.F. Bisson, C. Moreau, M. Dorfman, C. Dambra, and J. Mallon, Influence of Hydrogen on the Microstructure of Plasma-Sprayed Yttria-Stabilized Zirconia Coatings, *J. Therm. Spray Technol.*, 2005, **14**, p 85-90
8. D. Matejka and B. Benko, *Plasma Spraying of Metallic and Ceramic Materials*, John Wiley & Sons Ltd., Chichester, 1989, p 135
9. P. Saravanan, V. Selvarajan, M.P. Srivastava, D.S. Rao, S.V. Joshi, and G. Sundararajan, Study of Plasma- and Detonation Gun-Sprayed Alumina Coatings Using Taguchi Experimental Design, *J. Therm. Spray Technol.*, 2000, **9**, p 505-512
10. F. Gao, X. Huang, R. Liu, and Q. Yang, Development of the Process Index for NiCrAlY Coatings by the Mettech Axial III™ System, 2011, Unpublished Paper
11. J. Neter, W. Wasserman, and G.A. Whitmore, *Applied Statistics*, Allyn and Bacon, Inc., Boston, 1979
12. J.F. Li, H.L. Liao, C.X. Ding, and C. Coddet, Optimizing the Plasma Spray Process Parameters of Yttria Stabilized Zirconia Coatings Using a Uniform Design of Experiments, *J. Mater. Process. Technol.*, 2005, **160**, p 34-42
13. Y. Wang and T.W. Coyle, Optimization of Solution Precursor Plasma Spray Process by Statistical Design of Experiment, *J. Therm. Spray Technol.*, 2008, **17**, p 692-699
14. M. Friis, C. Persson, and J. Wigren, Influence of Particle In-Flight Characteristics on the Microstructure of Atmospheric Plasma Sprayed Yttria Stabilized ZrO_2, *Surf. Coat. Technol.*, 2001, **141**, p 115-127
15. R.J. Del Vecchio, *Understanding Design of Experiments: A Primer for Technology*, Hanser Publishers, Munich, 1997
16. H. J. Bajaria, *''Vital Few, Trivial Many''—Challenged, 52nd AQC 98 Transactions*, Philadelphia, May 5, 1998, p 1-7
17. C. Moreau, P. Burgess, and D. Ross, Characterization of Particle Flow in an Axial Injection Plasma Torch, *Thermal Spray Science and Technology*, ASM International, Materials Park, OH, 1995, *Proceeding of the 8th National Thermal Spray Conference*, Houston, September 11-15, 1995, p 141-147
18. J. Day, X. Huang, and N.L. Richards, Examination of Grit Blasting Process for Thermal Spraying Using Statistical Methods, *J. Therm. Spray Technol.*, 2004, **14**(4), p 471-479